

Optical spectrum of the IR-source IRC+10420 in 1992-1996

Klochkova V.G., Chentsov E.L., Panchuk V.E.

August 20, 2021

Special Astrophysical Observatory, Nizhnij Arkhyz, 357147 RUSSIA

Abstract

To understand the evolutionary stage of the peculiar supergiant IRC+10420, we have been taking spectra for several years at the 6 m telescope. The optical spectrum of IRC+10420 of the years from 1992 through 1996 points to the increase in the temperature: spectral class A5 instead of the former F8, as was pointed out by Humphreys et al., (1973). Now it resembles the spectra of late-type B[e] stars. The spectrum contains absorptions (mainly of ions) formed in the photosphere, apparently stationary with respect to the star center of mass, and emissions too, which can be formed in the fossil expanding envelope as well as partly in its compressing region.

Using our spectra and spectral data obtained by Oudmaijer (1995) we estimated the atmospheric parameters $T_{\text{eff}} = 8500$ K, $\log g = 1.0$, $\xi_t = 12$ km/s and concluded that metallicity of IRC+10420 is solar: the average value $[(V, Cr, Fe)/H]_{\odot} = -0.03$.

Combination of results allows us to consider IRC+10420 as a massive supergiant evolving to the WR-stage.

Keywords: – stars: evolution – stars: hypergiants – stars: individual: IRC+10420

1 Introduction

The OH/IR source IRC+10420 = IRAS19244+1115 identified with the peculiar high luminosity star V1302 Aql is a unique object, which has been carefully and comprehensively studied over the last decades but still remains a puzzle. Of the two hypotheses about its nature neither seems to be convincingly preponderant as yet. According to Fix and Cobb (1987), Hrivnak et al., (1989) and others this is a degenerate core giant evolving through the proto-planetary nebula stage with a luminosity no higher than $5 * 10^4 L_{\odot}$. According to Jones et al., (1993), Humphreys and Davidson (1994) and Oudmaijer et al. (1996) this is a core-burning hypergiant of $\approx 5 * 10^5 L_{\odot}$.

The difficulty of choice is due to:

- the uncertainty of fundamental observational parameters, such as spectral class and distance;
- the fact that with the difference in mass, age, even type of stellar population the evolutionary processes and their observational evidence are similar: in both alternatives the effective temperature of the star increases, there is a gaseous-dust envelope inherited from the red giant or supergiant phase, which interacts with the stellar wind;
- the presence of several competing models: thin chromosphere in the expanding gaseous-dust envelope such optically thick that we see the light of the star being multiple scattering by circumstellar dust (Fix and Cobb, 1987); a gaseous-dust disk in a clumpy envelope (Jones et al., 1993); jets with a small angle of opening (Oudmaijer et al., 1994); and at last infall of circumstellar material onto photosphere (Oudmaijer, 1995).

Outer regions of the source of radius 2-3 arcsec are mainly described and mapped by radio astronomy techniques from emission of molecules (paper by Nedoluha and Bowers (1992) and references therein). The gas envelope has been imaged by the methods of infrared speckle interferometry and coronagraphy (Ridgway et al., 1986OC; Kastner and Weintraub, 1995). The image of the dust envelope also extends to several seconds of arc, but the radiation is sharply enhanced in the region of

Table 1: Observation log of IRC+10420

Spectrum	Date	Spectral interval, Å
S03503	21.08.92.	5500-7200
S13003	11.12.95.	4800-6700
S13714	01.05.96.	5200-6800
S14409	03.07.96.	5200-7900

Table 2: Heliocentric radial velocities in km/s for groups of lines in the spectra of IRC+10420 in 1995-1996

Group of lines	n	V _r	
		em	abs
[OI], [CaII], [FeII]	6	+66 ± 2	
NI(3)	3		+66 ± 2
FeII(40,46)	7	+60 ± 3	
SiII(2)	2		+72 ± 2
ScII,TiII,CrII	6		≥+82 ± 2
FeII(48,49,74)	12	≤+40 ± 3	≥+91 ± 3
H _{α,β}	2	≤+15, +132	≥+71 ± 2
NaI(1), KI(1)	4		-5: +25:+(83-92)
DIB	11		-3 ± 2

about 0.1 arcsec in radius. However space or ground-based speckle images in the optical range, which could refine the structure of the central region, unknown to us.

Here the high resolution optical spectrum of IRC+10420, which contains the emission and absorption lines of the envelope and absorption ones of the photosphere or of the pseudophotosphere of the central star, is described.

2 Observational data

Spectra of IRC+10420 were taken with the CCD equipped echelle spectrometer LYNX mounted at the Nasmyth focus of the 6 m telescope of SAO RAS (Panchuk et al., 1993). The log of our observations is given in Table 1.

The average spectral resolution was 0.3 mÅ. The signal-to-noise ratio was equal to 20-50 for different spectral orders. Before 1995 a CCD of 530 x 580 pixels was used and the low echelle orders did not overlap, in the two latter spectra a CCD of 1140 x 1170 pixels was employed, and the indicated region overlapped completely. The MIDAS system was used for echelle-images reduction. The comparison spectrum source was an argon-filled thorium hollow-cathode lamp. Control and correction of instrumental displacement of the comparison and object spectra were done by the telluric lines O₂ and H₂O. The final accidental radial velocity determination errors are listed in Table 2. Systematic errors may reach 1-2 km/s.

3 Results and discussion

The only difference between the IRC+10420 spectra of 1992 and 1995-1996 we have noticed is the enhanced emission lines. Some emission lines, in particular close to λλ 6963, 7065, 7382, 7502, 7722 ÅÅ, distinctly shown in our last spectrum S14409 were absent both in our 1992 spectrum and in Oudmajer's spectrum which was obtained in 1994.

The spectral lines are united in groups by likeness of the profiles and closeness of the radial velocity values. The averaged profiles derived from the spectra S13714 and S14409 of higher quality for individual typical lines are shown in Fig. 1. The heliocentric radial velocities for the emission and absorption components of the profiles separately, also averaged over the groups of lines, are given in Table 2. In the second column of Table 2 are presented the numbers of lines in the groups, which were used for radial velocity measurements. As it is seen from Fig. 1, the line profiles are very different - from slightly asymmetric emissions details to undistorted absorptions lines through more complex intermediate forms. The variations in the shape of our line profiles follow the variations in the optical and IR lines according to Oudmaijer et al. (1994), and Oudmaijer (1995).

When comparing our radial velocity values with the data of other authors, aside from the profile variation from line to line and temporal variations it is necessary to take into account their asymmetry. It is relatively simple to compare more or less pure emission and absorption lines. The emission lines (first and third entries of Table 2) give $V_r = +(60 - 66)$ km/s, which is correlated with $+(61 - 65)$ km/s obtained from the optical, IR and radio emission lines (Olofsson et al., 1982; Fix and Cobb, 1987; Jones et al., 1993; Oudmaijer, 1995; Oudmaijer et al., 1996) and regarded usually as a "systemic velocity". For the absorption lines the agreement is worse: ours $+66$ km/s for NI(3) and $+72$ km/s for SiII(2) and $+74$ and $+78$ km/s, respectively from Oudmaijer (1995). The difference is likely to be connected with both different measuring methods and temporal variability.

For the asymmetric lines, in Table 2 are presented the radial velocities obtained from the peaks of the emissions details or from the cores of the absorption lines, the symbol \leq and \geq in front of them shows the type of asymmetry. The type of asymmetry as a rule is the same as in Oudmaijer (1995). The double-peaked structure of the emission lines H_α and H_β is likely to be followed in some ion lines as well, in particular, in the profiles of FeII(74) one can suspect a weak emission component with $V_r = +120 - 130$ km/s apart from the main peak with $V_r = +40$ km/s. On the other hand in the absorption lines of FeII (42) and part of lines ScII, TiII, CrII the small redshift of the wings with respect to the cores is apparently due to the presence of a blueward-shifted emission component.

The relation between velocity and line strength (Oudmaijer, 1995) one can reveal from our data too. The "pure" emissions of multiplets 40 and 46 of FeII show the radial velocities from $+55$ km/s for the strongest line $\lambda 6516\text{\AA}$ to $+64$ km/s for the weakest one $\lambda 6116\text{\AA}$ and velocities measured for the members of multiplet 73 change from $+40$ km/s to $+63$ km/s.

Note also that in the deepest part of the absorption of NaI and KI two main components with $V_r \approx -5$ km/s and $\approx +25$ km/s are recognized. Both of them, at least the first one, are interstellar completely or to a considerable degree: the lines NaI and CaII in the spectra of early type stars in the vicinity of IRC+10420 show close radial velocities. In particular, one of those stars is heavily reddened supergiant HD 183143 B7Iae. Interstellar absorptions of KI in its spectra consist of two components of almost equal intensity with the radial velocities about -11 and $+4$ km/s (Chaffee and White, 1982; Herbig and Soderblom, 1982). By our resolution they correspond to the values in the two last entries in Table 2. The likeness between the blue part of the NaI line profile and profiles of diffuse interstellar bands in the spectrum of IRC+10420 (both in a shape and velocity) is noticeable. But it is necessary to keep in mind that the DIB possess intrinsic (not kinematic) asymmetry as well.

Can any of the radial velocity values that we have obtained be referred to the center of mass of the star? Apparently only those that have been measured from both almost symmetric emission and absorption lines (entries 1-3 of Table 2). One can consider also different, more complex lines as a natural consequence of superposition of non-shifted photospheric absorption lines and "inverse P Cyg profiles" with blue-shifted emission and red-shifted absorption features.

When considering IRC+10420 as a massive star, it is necessary that its velocity should be matched with its distance. The galactic longitude of our object is such ($l = 47^\circ$) that it falls nearly in the center of the 30° window free from associations and poor in bright supergiants and O-stars (Humphreys, 1978). The line of sight passes between the Car-Sgr arm and its local branch (e. g. see Fig. 7 in Myers et al. (1986)). Coupled with the strong reddening, this suggests that the object is very distant. But even at the tangent point (distance of about 7 kpc) its heliocentric radial velocity produced by

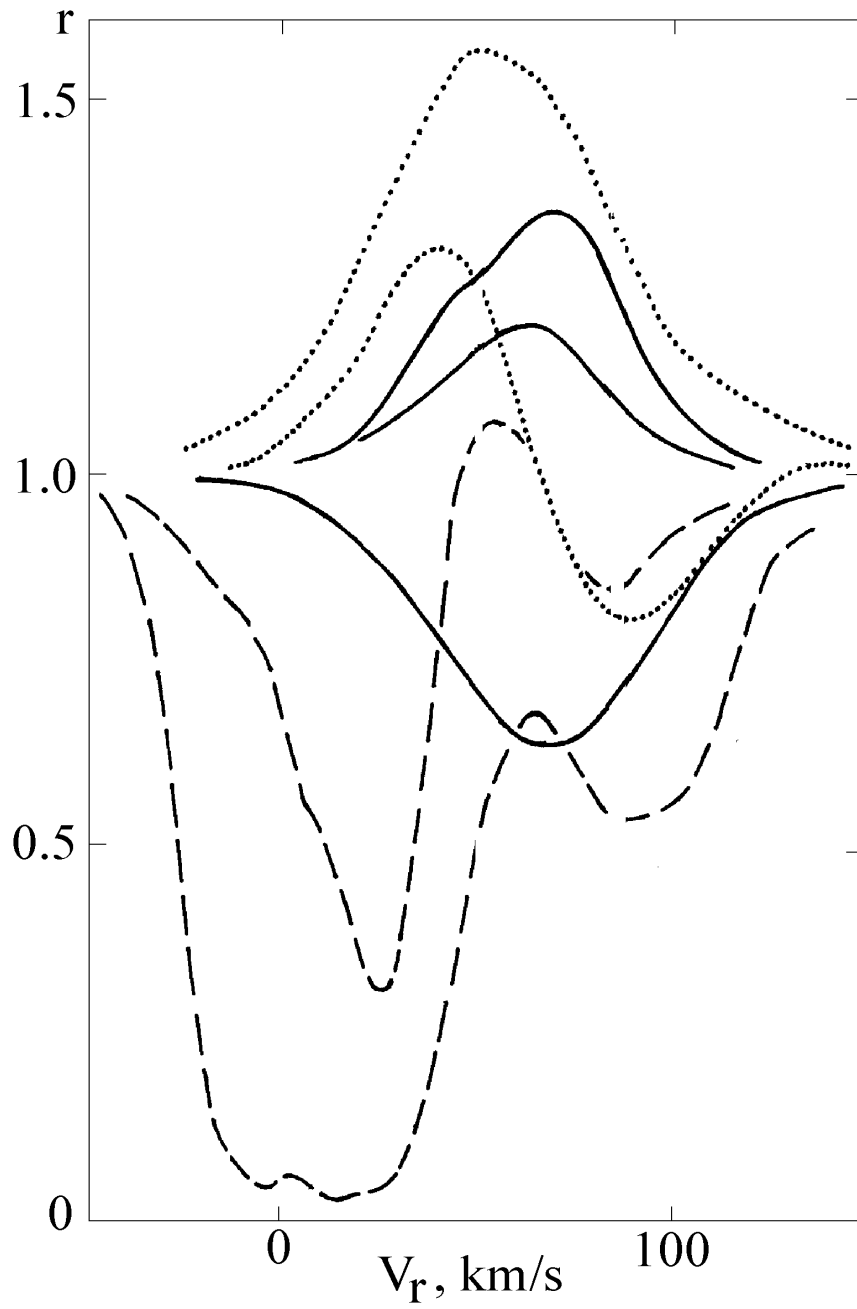


Figure 1: Line profiles in the optical spectrum of IRC +10420. From top to bottom: dotted lines - FeII(40) 6432, FeII(74) 6456; solid lines - [FeII] 14F 7155, [OI] 1F 6300, NI(3) 7468; dashed lines - KI(1) 7699, NaI(1) 5890.

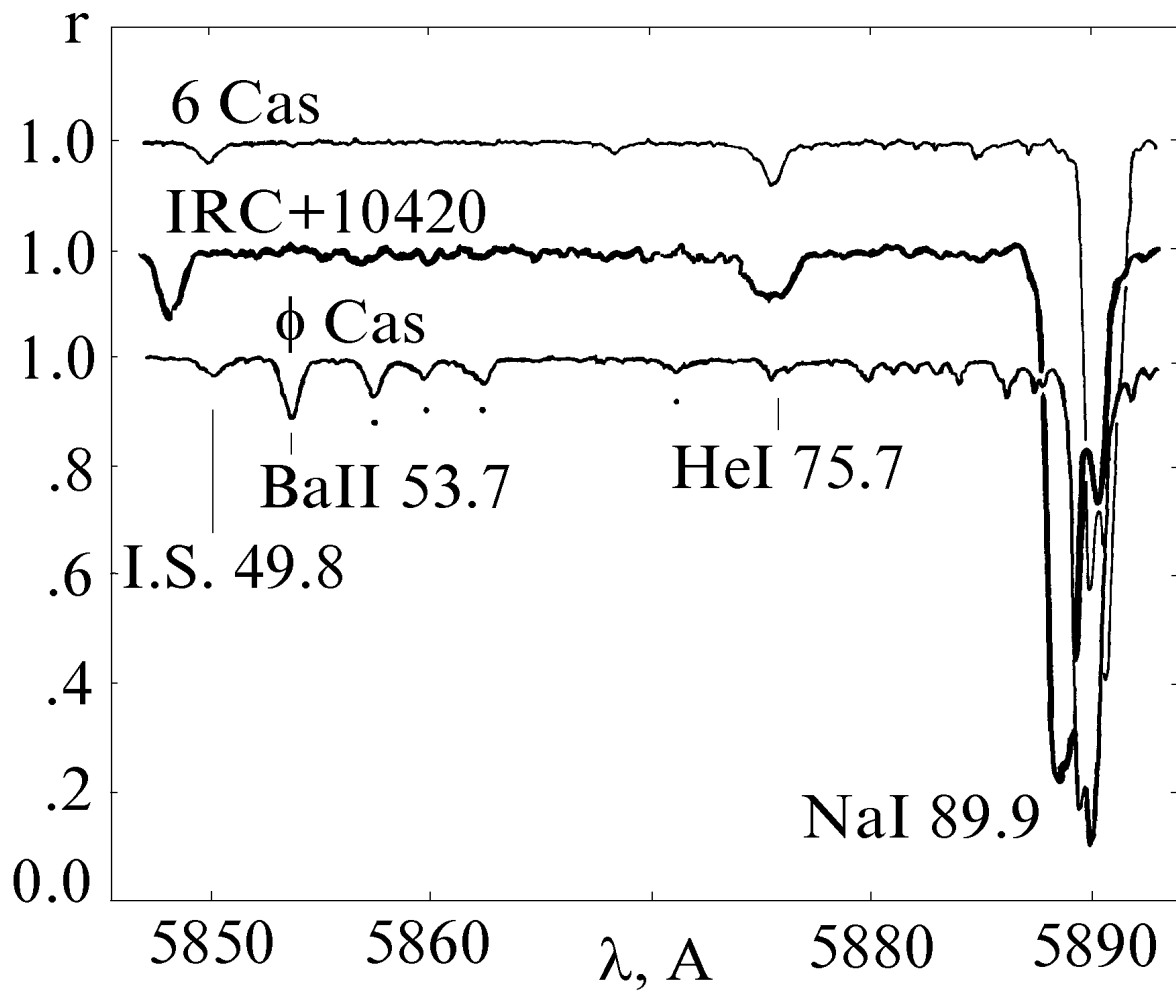


Figure 2: Comparison of the IRC +10420 spectrum into the region 5848 – 5894 \AA with that for supergiants 6 Cas A2.5 Ia-0 and ϕ Cas F0Ia. Absorption lines of neutral metals (mainly - FeI) are marked by dots.

differential rotation is no higher than 60 km/s, which is slightly less than the velocities obtained both from lines with minimal asymmetry and IR and radio data.

The latter fact together with "inverse P Cyg profiles" of many lines, as well the character of their temporal variations according to Oudmaijer (1995) (both emission and absorption components become stronger or grow weak simultaneously) could be regarded as evidence of accretion. But it should be noted also and some difficulty of this conception. Indeed, normal P Cyg profiles has been recorded by Fix and Cobb (1987) and by Oudmaijer (1995) for the IR line of CO, which is formed in the extended fossil envelope. The blue shift of the absorption core with respect to the emission peak suggests that the envelope is expanding at a velocity of 40 km/s. Close values, from 40 to 50, are obtained also from the widths of the envelope emissions in our spectra. It is in good agreement with the data of other authors obtained in both the optical and the IR, and radio wavelength ranges. One should not exclude that the lines of NaI(1) and KI(1) also contain ordinary P Cyg-profiles superimposed on photospheric absorptions and distorted by the interstellar components. The values close to 40 km/s are obtained from the widths of the molecular and forbidden atomic emission lines. As it is obvious both from our Fig. 1 and Oudmaijer's data (1995), these values for permitted emission lines are even greater. But the interpretations of the line broadening are opposite: expansion for the forbidden lines and compression for the permitted ones. According to such a model the profiles for the forbidden emission lines are shaped by matter going both up and down consequently by matter immobile relative to the star. However, these profiles have not any narrow details to mark the velocity of the star center of mass. We have no distinct impression that the red wings of photospheric absorption lines contain the strong envelope components. At least, the latter do not prevent from the quantitative spectral classification.

Humphreys et al. (1973) was the first to estimate the spectral class of IRC+10420 as F8I. Since then and until recently (Oudmaijer, 1995; Oudmaijer et al., 1996) it has apparently never been revised, although Fix (1981) has noted that the absorption lines in IRC+10420 are weaker than in γ Cyg F8Ib. This estimate is one of the signs that IRC+10420 is similar to the unique object η Carinae, which also showed the spectrum of an F-supergiant in 1893 (Walborn and Liller, 1977). Over the last 20 years the expected rise in temperature of IRC+10420 has actually taken place, not as great as in η Carinae though. Fig. 2 shows that in 1995-1996 the object IRC+10420 is much closer to 6 Cas A2.5 Ia-0 in spectrum than to ϕ Cas F0 Ia - the absorptions of the neutral metals are absent, but the HeI line $\lambda 5876\text{\AA}$ can be seen. We estimate the spectral class of IRC+10420 using spectral criteria developed for high-dispersion spectra of normal supergiants and for both blue and red lines (data by Oudmaijer (1995) and our own, respectively). Our evaluation of spectral class is A5 with the spread from A3 to A7 for individual criteria.

The rise in effective temperature in IRC+10420 allows us to more seriously treat its likeness to, possibly, even a relationship with B[e] supergiants. In the last time the domains of this group has been extended in luminosity from 10^6 to $10^4 L_{\odot}$ and to B9 in spectral class. The main thing is that spectra have been obtained in which the absorptions show small, occasionally even red shifts with respect to the emission features (Zickgraf et al., 1992; Gummertsbach et al., 1995). Moreover, on the (J-H)-(H-K) diagram IRC+10420 falls within the same isolated region that is occupied by B[e] stars due to their IR excess.

4 Estimation of metallicity

For understanding of an object at an unclear evolutionary stage, it is very important to know its metallicity and chemical abundance pattern.

To study in detail the chemical composition of an unstable supergiant with the presence of strong gradient of radiative pressure and velocity field, one can not use classical model atmospheres method. One needs dynamic inhomogeneous spherical models in this case. Therefore it should be noted that we present here the preliminary results only on chemical composition of IRC+10420 because we use

the standard plane-parallel homogeneous models grid of Kurucz (1979).

For chemical composition calculation by the model atmosphere method, one needs to know the values of the effective temperature T_{eff} , surface gravity $\log g$ and microturbulent velocity ξ_t . The most difficult problem is effective temperature determination. Determination of T_{eff} is problematic even for normal supergiants due to their extended atmospheres and significant non-LTE effects (Venn, 1993, 1995a,b). The problem arises for such a peculiar star as IRC+10420, for which the energy distribution is strongly distorted by interstellar and circumstellar extinction. We can not use also in the case of IRC+10420 the equivalent widths and profiles of hydrogen lines for T_{eff} and $\log g$ determination. These spectral features being well known criteria of atmospheric conditions for the atmospheres of normal A-supergiants are hardly distorted in the spectrum investigated.

Table 3: Atomic data, equivalent widths W of lines in the spectrum of IRC+10420

$\lambda, \text{\AA}$	Species	EP, ev	$\log gf$	$W, \text{m\AA}$	$\epsilon(X)$
5172.70	Mg	2.71	-.38	184	7.42
4128.05	Si+	9.84	.57	237	7.05
5978.93	Si+	10.07	-.06	101	7.16
4325.01	Sc+	.60	-.44	230	3.51
4400.36	Sc+	.61	-.63	226	3.69
5239.81	Sc+	1.45	-.77	53	3.51
5526.79	Sc+	1.77	.13	180	3.47
5640.99	Sc+	1.50	-1.01	30	3.49
5657.91	Sc+	1.51	-.50	178	3.90
5667.15	Sc+	1.50	-1.20	15	3.36
5669.04	Sc+	1.50	-1.09	38	3.68
5684.20	Sc+	1.51	-1.01	22	3.35
4028.33	Ti+	1.89	-1.12	169	5.00
4287.89	Ti+	1.08	-1.68	185	5.02
4316.81	Ti+	2.05	-1.52	57	4.87
4386.86	Ti+	2.60	-1.11	141	5.31
4411.08	Ti+	3.09	-.82	131	5.31
4411.94	Ti+	1.22	-2.32	66	5.17
4421.95	Ti+	2.06	-1.43	112	5.13
4464.46	Ti+	1.16	-1.78	180	5.14
4470.86	Ti+	1.16	-2.00	119	5.11
4488.32	Ti+	3.12	-.86	156	5.47
4529.47	Ti+	1.57	-1.93	59	4.95
4544.01	Ti+	1.24	-2.28	43	4.92
4568.31	Ti+	1.22	-2.52	32	5.01
4779.98	Ti+	2.05	-1.37	125	5.09
4805.10	Ti+	2.06	-1.05	198	5.06
4874.01	Ti+	3.09	-.79	120	5.19
4911.18	Ti+	3.12	-.34	190	5.05
5129.16	Ti+	1.89	-1.39	192	5.24
5185.90	Ti+	1.89	-1.35	170	5.12
5211.53	Ti+	2.59	-1.85	40	5.33
5336.78	Ti+	1.58	-1.70	114	5.00

5381.01	Ti+	1.57	-2.08	76	5.16
3951.97	V +	1.48	-.52	235	4.16
4023.39	V +	1.80	-.72	95	3.99
4600.19	V +	2.27	-1.31	16	3.98
4252.62	Cr+	3.86	-2.10	78	5.78
4261.92	Cr+	3.86	-1.73	154	5.81
4269.28	Cr+	3.85	-2.33	87	6.06
4275.57	Cr+	3.86	-1.85	186	6.05
4284.21	Cr+	3.85	-1.91	105	5.75
4555.02	Cr+	4.07	-1.45	228	5.93
4592.07	Cr+	4.07	-1.35	239	5.88
4616.64	Cr+	4.07	-1.35	173	5.62
4812.35	Cr+	3.86	-1.89	67	5.46
5279.88	Cr+	4.07	-2.10	37	5.50
5308.46	Cr+	4.07	-1.81	48	5.34
5313.61	Cr+	4.07	-1.65	120	5.66
5334.88	Cr+	4.07	-1.89	126	5.92
4045.82	Fe	1.48	.28	215	7.37
4063.60	Fe	1.56	.06	93	7.11
4071.74	Fe	1.61	-.01	107	7.29
4132.06	Fe	1.61	-.63	43	7.44
4181.76	Fe	2.83	-.31	24	7.67
4210.35	Fe	2.48	-.95	15	7.86
4250.13	Fe	2.47	-.41	10	7.12
4250.79	Fe	1.56	-.73	63	7.68
4271.16	Fe	2.45	-.35	16	7.26
4271.76	Fe	1.48	-.16	92	7.25
4325.76	Fe	1.61	-.02	175	7.57
4383.55	Fe	1.48	.20	222	7.44
4404.75	Fe	1.56	-.14	144	7.53
4122.67	Fe+	2.58	-3.62	158	7.47
4128.74	Fe+	2.58	-4.00	100	7.56
4273.32	Fe+	2.70	-3.53	123	7.28
4541.52	Fe+	2.86	-3.21	218	7.44
4582.84	Fe+	2.84	-3.44	131	7.30
4620.51	Fe+	2.83	-3.61	78	7.16
4666.75	Fe+	2.83	-3.57	117	7.35
6247.55	Fe+	3.89	-2.51	192	7.30
6456.39	Fe+	3.90	-2.30	234	7.27
4077.71	Sr+	0.00	0.21	253	2.63
4215.52	Sr+	0.00	0.04	140	2.36
4177.54	Y +	0.40	-0.24	177	3.28
4398.02	Y +	.12	-.14	52	2.28
4149.20	Zr+	.79	-.13	85	2.97

We can use the spectroscopic method of temperature determination only, forcing independence of the abundance derived for each line upon the excitation potential of the low level for this line. The parameter $\log g$ was estimated through ionization balance for FeI and FeII. The microturbulent velocity value based on W of CrII, FeII, ScII and TiII lines is very high and equal to 12 km/s. But such a high, close to the velocity of sound, value of microturbulent velocity is trivial for the most luminous hot supergiants at the limit of the HR-diagram (Nieuwenhuijzen, de Jager, 1992).

It is well known that the plane-parallel static model atmosphere method does not give correct abundances for high luminosity stars, (Ia, Ia+). The profiles of the spectral lines observed are additionally broadened by non-thermal mechanisms whose influence may be variable at different levels in the atmosphere. To obtain more reliable estimates of abundances we use only weak lines with $W < 250 \text{ m\AA}$. Such lines formed closer to photospheric layers are more correctly described by a standard stationary model.

All lines which have been used for chemical composition calculation are listed in Table 3. Here are given also equivalent widths W , oscillator strengths $\log gf$ used, excitation potentials EP of lower level and abundances calculated for individual lines. It should be noted that for abundance calculations we used equivalent widths derived from both our spectra of IRC+10420 and the spectrum kindly provided by R.Oudmaijer. For most lines our W coincided with that measured by Oudmaijer (1995).

The model atmosphere parameters and abundances of several chemical elements obtained are presented in Table 4. The abundances are given on the scale $\epsilon(X) = \log N(X) - \log N(\text{H})$, at $\log N(\text{H}) = 12.0$.

The value for $T_{\text{eff}} = 8500 \text{ K}$ derived from the intensity of neutral iron absorption lines is well fit for the value of spectral class $A5 \pm 0.5$ determined from the W of a sample of lines of different chemical elements (FeII, CrII, TiII). The internal uncertainty of the main model parameter T_{eff} is equal to $\Delta T_{\text{eff}} = \pm 250 \text{ K}$, which corresponds to the accuracy of spectral classification. The error of the $\log g$ value derived from ionization equilibrium of iron is determined by forcing a maximum difference between $\epsilon(\text{FeI})$ and $\epsilon(\text{FeII})$ of 0.1 dex. Such difference is achieved by varying of $\log g$ by ± 0.2 at other constant parameters (T_{eff} and ξ_t). The value of ξ_t is determined with an uncertainty of $\pm 1.0 \text{ km/s}$, which is typical for A-supergiants (Venn, 1993). The calculated abundance errors caused by uncertainties of the atmospheric parameters T_{eff} , $\log g$ and ξ_t are given in Table 5. As it shown in this Table, the limitation of equivalent width of lines used $W < 250 \text{ m\AA}$ reduces significantly the influence of uncertainty of ξ_t choice. The main factor of abundance errors for most species is the uncertainty of T_{eff} value.

As it is shown in Figure 3, there is no relationship between $\epsilon(\text{Fe})$ and equivalent widths W and excitation potentials EP of iron lines which have been used for metallicity estimation of IRC+10420. It illustrates sufficiently correct choice of model parameters.

A lot of absorption lines of ionized metals (Ti, Sc, Cr) have been reliably measured in the spectrum of IRC+10420. It is important that we have not found any dependence of abundance of these ions neither on W or EP. Therefore the microturbulent velocity does not vary between different chemical elements.

As it is shown in Table 4, abundances of a number of species (ScII, TiII, VII, CrII, FeI, FeII) are determined with a high internal accuracy, $\pm \sigma \leq 0.03 - 0.06$. It allows us to conclude that with a high probability the metallicity for IRC+10420 is close to solar: the average abundance for elements of iron-group relative to the Sun is $\epsilon(\text{V}, \text{Cr}, \text{Fe}) = -0.03$.

The α -process element silicon is underabundant, at the same time the ScII abundance well determined from 9 lines is increased relative to Fe: $[\text{Sc}/\text{Fe}]_{\odot} = +0.49 \text{ dex}$. The derived underabundance of silicon may be real and caused by the selective depletion of a part of this chemical element due to condensation to silicate dust in the circumstellar envelope and following accretion of such "cleaned" gas onto the photosphere. Similar processes are known for stars with IR-excesses: λ Bootis stars (Venn, Lambert, 1990; Stürenburg, 1993) and post-AGB stars (van Winckel, 1997). In connection with the silicon photospheric underabundance it should be noted that the spectral energy distribution (SED) of IRC+10420 fits to a two-component shell model, and SED for the inner hotter shell fits to **silicate** dust (Oudmaijer et al., 1996).

Individual abundances of the heavy s-process metals Sr, Y, Zr are determined with a large error because of the small number of lines measured. But the average abundance close to the solar value of $[\text{X}/\text{Fe}]$ for these s-process metals is sufficiently reliable.

All these details of chemical composition for IRC+10420 is similar to the average chemical composition of massive A-supergiants (Venn, 1995a).

Unfortunately, within the frames of standard models, we can not derive quantitative conclusions

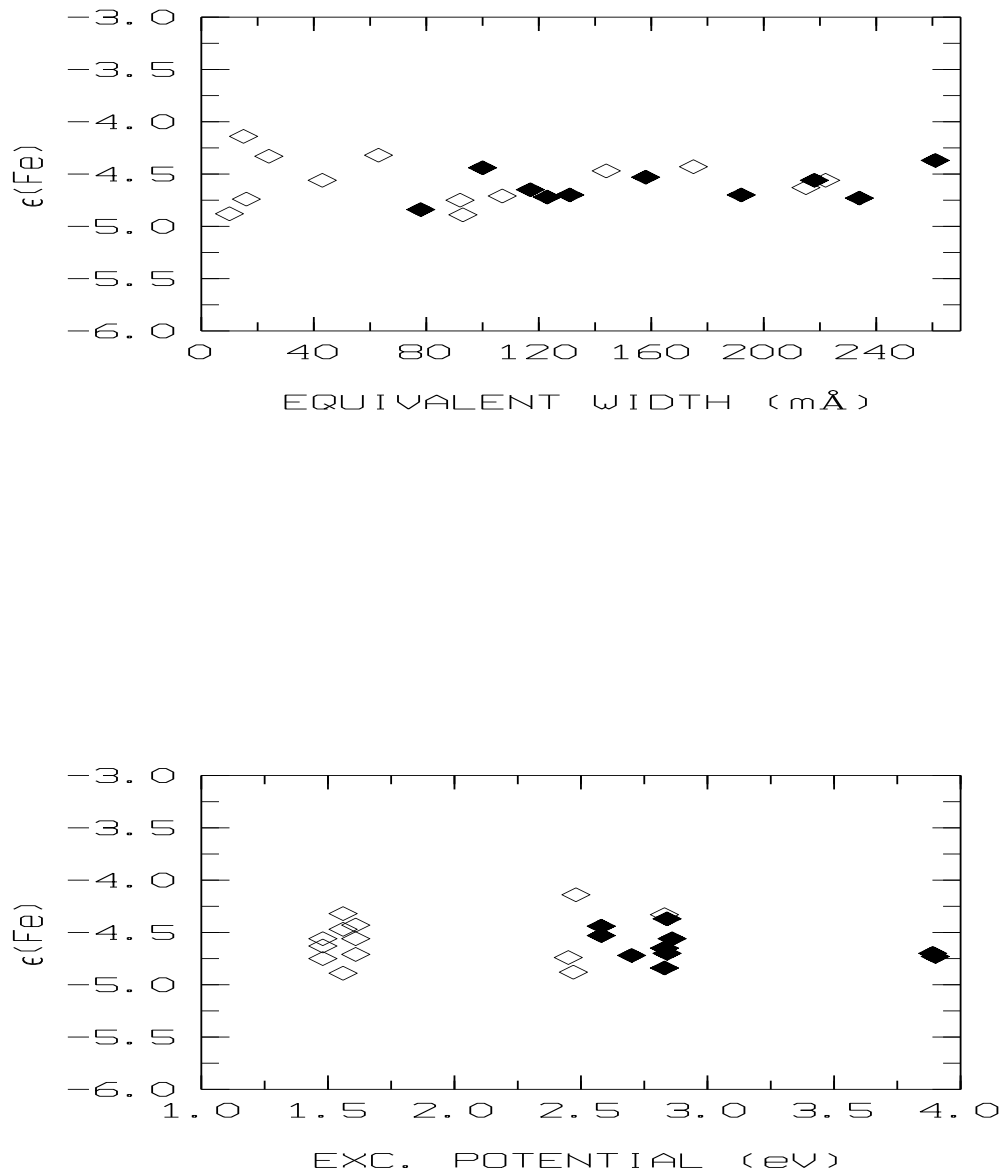


Figure 3: Iron abundance derived from individual FeI (open symbols) and FeII (filled symbols) lines as a function of line equivalent width W (upper panel) and as a function of excitation potential (lower panel).

Table 4: Model atmosphere parameters adopted and abundances of chemical elements for IRC+10420. $\log N(\text{H}) = 12.0$. n - number of lines used for calculation. The data by Grevesse and Noels (1993) are adopted for solar abundances.

$T_{\text{eff}} = 8500 \text{ K}, \log g = 1.0, \xi_t = 12 \text{ km/s}$				
Element	$\epsilon(\text{X})$	$\pm\sigma$	n	$[\text{X}/\text{H}]_{\odot}$
MgI	7.42		1	-0.12
SiII	7.10	0.06	2	-0.45
ScII	3.55	0.06	9	+0.38
TiII	5.12	0.03	22	+0.10
VII	4.04	0.06	3	+0.04
CrII	5.76	0.06	13	+0.09
FeI	7.43	0.06	13	-0.07
FeII	7.35	0.04	9	-0.15
SrII	2.50		2	-0.40
YII	2.78		2	+0.54
ZrII	2.97		1	+0.37

Table 5: Estimated errors of chemical elements abundances due to uncertainties of the atmospheric parameters T_{eff} , $\log g$ and ξ_t .

Element	$\Delta(\text{X})$		
	$\Delta T_{\text{eff}} = -250 \text{ K}$	$\Delta \log g = +0.2$	$\Delta \xi_t = -1 \text{ km/s}$
MgI	-0.50	-0.25	0.03
SiII	+0.07	+0.10	0.06
ScII	-0.46	-0.15	0.01
TiII	-0.34	-0.10	0.01
VII	-0.29	-0.07	0.02
CrII	-0.18	-0.00	0.04
FeI	-0.51	-0.26	0.01
FeII	-0.17	-0.00	0.02

Table 6: Comparison of equivalent widths W of C,N-lines for two high luminous stars HD 13476 (Venn, 1995b) and IRC+10420 (Oudmaijer, 1995)

$\lambda, \text{\AA}$	$W, \text{m\AA}$	
	HD 13476	IRC+10420
CI:		
9088.57	240	67
9094.89	392	260
9111.85	240	68
NI:		
7423.63	95	288
7442.28	164	434
7468.29	214	604
8184.80	230	491
8187.95	251	518
8210.64	128	293
8216.28	358	779
8242.34	216	523
8629.24	269	312
8703.24	279	621
8711.69	306	590
8718.82	258	544
8728.88	91	211

concerning nitrogen and oxygen content for IRC+10420 because in its spectrum only very strong lines of these elements are observed, with $W > 300 - 400 \text{ m\AA}$. To obtain reliable abundances of these elements the LTE-approach is insufficient for the case of A-supergiants (Venn, 1995b).

But we can draw qualitative conclusions about the behaviour of C, N-lines in the IRC+10420 spectrum from a comparison of their equivalent widths with ones for normal supergiants of similar effective temperature and surface gravity. We have used for the comparison the equivalent widths of carbon and nitrogen lines in the spectrum of the massive supergiant HD 13476 (A3Iab) for which Venn (1995a) has derived atmospheric parameters: $T_{\text{eff}} = 8400 \text{ K}$, $\log g = 1.2$, $\xi_t = 8 \text{ km/s}$. Abundances of some metals for HD 13476 are solar and very close to that of IRC+10420 estimated here. Later Venn (1995b) calculated non-LTE C-, N-abundances for 22 A-type supergiants including HD 13476. Carbon and nitrogen relative to the iron content for HD 13476 $[\text{C}/\text{Fe}]_{\odot} = -0.43$, $[\text{N}/\text{Fe}]_{\odot} = 0.08$ are close to the averages for the whole sample studied. The non-LTE corrections are vary: $\Delta = -0.42$ for carbon and $\Delta = -0.80$ for nitrogen. The value $[\text{N}/\text{C}]_{\odot} = 0.51$ is very similar to the first dredge-up for stars with mass near $8 - 10 M_{\odot}$.

The equivalent widths of N lines in the spectrum of IRC+10410 are much stronger (2-3 times) in comparison to the W -values of the same lines in the HD 13476 spectrum and the equivalent widths of C lines are essentially weaker (see Table 6). Therefore we can conclude that $[\text{N}/\text{C}]_{\odot}$ -value for IRC+10420 in any case is not less than that for HD 13476.

5 Conclusions

So, the optical spectrum of IRC+10420 of the years from 1992 through 1996

- points to the increase in the temperature: spectral class A5 instead of F8 in 1973;

- contains absorptions (mainly of ions) formed in the photosphere, apparently stationary with respect to the star center of mass;
- contains emission details too, which are formed in the expanding envelope and perhaps in its compressing layers;
- resembles the spectra of late-type B[e] stars;

The metallicity, which is close to solar, and the altered [N/C]-value allow us to consider IRC+10420 as a massive object at the evolution stage of at least after the first dredge-up and not to reject the hypothesis of Jones et al. (1993) who suggested that IRC+10420 is a true hypergiant with a mass of about $40 M_{\odot}$, evolving from the red supergiant phase to the Wolf-Rayet stage.

The nature of IRC+10420 is still open question. New observations are necessary to obtain full chemical abundance pattern and to coordinate luminosity, distance and radial velocity of this object. Besides that we need more careful identification of extremely plentiful and variable features of the optical spectra of IRC+10420. For example, what are the enigmatic narrow strong absorption details $\lambda\lambda$ 5694, 6286, 6288 Å ? For the present one can say only that these are not telluric lines.

It should be noted that in the frames of the study of supergiants with infrared excess (Klochkova, 1995; Začs et al., 1995) we have obtained also the spectra of the supergiant HD179821 = IRAS19114+0002, which has been considered analogous to IRC+10420 (Kastner, Weintraub, 1995). Based on these spectra results have recently been obtained (Záčs et al., 1996) for HD179821, using the model atmosphere method: $T_{\text{eff}} = 6800$ K, $\log g = 1.3$, iron peak elements are slightly underabundant, Sc and Ti are slightly overabundant. But for this object Začs et al. (1996) revealed the overabundance of sodium, s-process (Y, Zr) and r-process (Eu) elements. The overabundance of s-process points to the post-AGB stage of evolution of HD 179821. However for more general conclusions about the nature of HD 179821 and its likeness to IRC+10420, abundances of CNO-triad are needed.

Acknowledgements. We thank Prof. Yu.N.Efremov for helpful discussion on localization of IRC+10420 in the Galaxy and Dr. R. Oudmaijer for a part of his Ph.D. Thesis kindly made available to us. We are also indebted to the referee for detailed and fruitful discussion and suggestions.

Program of spectroscopic research of IRAS-sources has financial support from the Russian Federal Program "Astronomy". We acknowledge also the partial support from KBN grant No.2P03D.026.09.

References

- [1] Chaffee F.H., White R.E. 1982. ApJS, 50, 169
- [2] Fix J.D. 1981, ApJ, 248, 542
- [3] Fix J.D., Cobb M.L. 1987, ApJ, 312, 290
- [4] Grevesse N., Noels A. 1993. In: Origin and Evolution of the Elements. Eds. N. Prantzos, E. Vangioni-Flam and M. Gasse. Cambridge University Press, p.14
- [5] Gummersbach C.A., Zickgraf F.-J., Wolf B. 1995, A&A, 302, 409
- [6] Herbig G.H., Soderblom D.R. 1982. ApJ, 252, 610
- [7] Hrivnak B.J., Kwok S., Volk K.M. 1989, ApJ, 346, 265
- [8] Humphreys R.M. 1978, ApJS, 38, 309
- [9] Humphreys R.M., Strecker D.W., Murdock T.L., Low F.J. 1973, ApJ, 179, L49
- [10] Humphreys R.M., Davidson K. 1994, PASP, 106, 1025
- [11] Jones T.J., Humphreys R.M., Gehrz R.D., Lawrence G.F., Zickgraf F.-J., Moseley H., Casey S., Glaccum W.J., Koch C.J., Pina R., Jones B., Venn K., Stahl O. and Starrfield S.G. 1993, ApJ, 411, 323
- [12] Kastner J.H., Weintraub D.A. 1995, ApJ, 452, 833

- [13] Klochkova V.G. 1995, MNRAS, 272, 710
- [14] Kurucz R.L. 1979, ApJ Suppl, 40, 1
- [15] Myers P.C., Dame T.M., Thaddeus P., Cohen R.S., Silverberg R.F., Dwek E., Hauser M.G. 1986, ApJ, 301, 398
- [16] Nedoluha G.E., Bowers P.F. 1992, ApJ, 392, 249
- [17] Nieuwenhuijzen H., de Jager C. 1992. In: Instabilities in evolved super- and hypergiants. North-Holland, Amsterdam/Oxford/New York/Tokyo. Eds. C. de Jager and H. Nieuwenhuijzen. P.127
- [18] Olofsson H., Johansson L.E.B., Hjalmarson A., Nguyen-Quang-Rieu, 1982, A&A, 107, 128
- [19] Oudmaijer R.D. 1995. Ph.D. Thesis.
- [20] Oudmaijer R.D., Geballe T.R., Waters L.B.F.M., Sahu K.C. 1994, A&A, 281, L33
- [21] Oudmaijer R.D., Groenewegen M.A.T., Matthews H.E., Blommaert J.A.D.L., and Sahu K.C. 1996, MNRAS, 280, 1062
- [22] Panchuk V.E., Klochkova V.G., Galazutdinov G.A., Ryadchenko V.P., Chentsov E.L. 1993, SvA, 19, L1061
- [23] Ridgway S.T., Joyce R.R., Connors D., Pipher J.L., Dainty Ch. 1986 ApJ, 302, 662
- [24] Stürenburg S. 1993, A&A, 277, 139
- [25] Venn K.A. 1993, ApJ, 414, 316
- [26] Venn K.A. 1995a, ApJS, 99, 659
- [27] Venn K.A. 1995b, ApJ, 449, 839
- [28] Venn K.A., Lambert D.L. 1990, ApJ, 363, 234
- [29] Walborn N.R., Liller M.H. 1977, ApJ, 211, 181
- [30] van Winckel H. 1997, A&A, 319, 561
- [31] Začs L.A., Klochkova V.G., Panchuk V.E. 1995. MNRAS, 275, 764
- [32] Začs L.A., Klochkova V.G., Panchuk V.E. and Spēlmanis R. 1996. MNRAS, 282, 1171
- [33] Zickgraf F.-J., Stahl O., Wolf B. 1992, A&A, 260, 205